

Continuous Monitoring of Organic Pollutants in Water by Sparging-Infrared

Walter M. Doyle

This paper reviews the new field of sparging-infrared waste water analysis, first outlining the theoretical basis for the technique and then providing experimental examples illustrating its operation. The key to the high sensitivity of sparging-infrared is the highly favorable partitioning that occurs, in equilibrium, between the vapor and liquid phases of typical organic pollutants. This can result in a four to five order of magnitude enhancement of the ratio of solute concentration to water concentration in the vapor phase compared to the liquid phase, enabling highly sensitive measurements to be made in an infrared gas cell. Detection limits are typically in the low parts per billion range for the substances of greatest environmental concern.

1. Introduction

Sparging-IR is a new technique for the rapid analysis of organics dissolved in water. Its development has been driven by the need to detect leaks or spills in industrial plants at an early stage so as to allow a stream to be diverted to a holding tank or remediation facility until the problem is solved. In this light, the goal has been the development of a process instrument capable of preventing discharge into the environment rather than simply detecting it after it has occurred. This necessitates essentially real-time operation and thus precludes the use of the chromatographic techniques commonly used for compliance monitoring.

At first thought, Fourier transform infrared (FT-IR) spectroscopy might not seem like a likely candidate for use in a sensitive real-time waste water analyzer. For one thing, FT-IR has a limited dynamic range and thus is generally not thought of as a trace detection method. Secondly, water is a strong IR absorber, with broad bands spanning the fingerprint spectral region. These factors limit the ability of FT-IR to measure the concentrations of organics in liquid water. However, the use of the sparging technique in conjunction with FT-IR changes this situation dramatically.

The basis for the sparging-IR technique is the establishment of a condition of dynamic equilibrium between the concentra-

tions of solutes in a stream of water and their vapor pressures in a sparging air stream. The vapor concentrations are then measured by means of an FT-IR spectrometer and a gas transmission cell. The measured vapor concentrations are related to the liquid concentrations by the ideal gas law and Henry's law governing the vapor pressures of solutions. An important characteristic of this approach is that the vapor phase concentrations are proportional to the fractional saturation in the liquid phase rather than the fractional concentration. This results in a marked enhancement of measurement sensitivity for weakly soluble substances. For many substances, the relative concentrations in the vapor phase can be enhanced as much as four or five orders of magnitude compared to their liquid phase concentrations.

The sparging-IR technique was pioneered at E.I. DuPont by S.W. Fleming, who developed a continuous on-line system for the analysis of chlorinated hydrocarbons in waste water (1). This system, which has been operating continuously for over a year as of this writing, employs a closed loop air stream to provide dynamic equilibrium partitioning between the liquid and vapor phases.

More recently, two commercial sparging-IR systems have been developed: a large scale system intended for continuous on-line use (2,3,4) and a smaller bench top system for laboratory or near line sampling (5). Both of these systems can be operated with either closed or open loop air flow and either a continuously flowing waste water stream or a static sample. Two modes of operation, closed loop continuous flow and open loop static sample, are particularly attractive and, in fact,

The author is with Hellma Axiom, 1451-A Edinger Ave, Tustin, California 92780. W.M. Doyle's e-mail address is michael.doyle@hellma.com.

tend to compliment each other. The unique features of each will be discussed below.

2. Basic Principles

The operation of the sparging-IR system can be best understood if we first consider what happens when a sample of contaminated water is left standing in a closed vessel. Both water and solute molecules will evaporate from the liquid surface giving rise to build up of vapor pressure in the head space. This process will eventually come to equilibrium when the rate of condensation becomes equal to the rate of evaporation. At this point, the partial pressure of each species will depend only on its liquid phase concentration, its inherent vapor pressure, and its solubility, allowing the concentration in the liquid to be measured by simply measuring the vapor pressure in the head. Indeed, head space GC is one of the techniques currently used for the analysis of static waste water sample.

Sparging, (ie. passing a stream of air bubbles through volume of water), can be thought of as simply a means of accelerating the transition to equilibrium. This occurs because of the very high ratio of surface area to volume in the minute air bubbles. Of course, the evaporation process does partially deplete the concentration of solute in the water. However, the effect of this on the measurement can be minimized by using countercurrent flow with a relatively high ratio of water flow rate to air flow rate. Furthermore, the effect can be completely eliminated by continuously circulating the same volume of air through the system. In this “closed loop” mode of operation, the calibration of the system for a given species will depend only on the pollutant’s equilibrium vapor pressure and solubility, the length of the gas cell, temperature, and the fixed characteristics of the calibration matrix. In the open loop mode, the calibration will also depend on the ratio of the air and water flow rates. This latter dependence is most significant for weakly soluble species.

The performance of the sparging-IR system is enhanced significantly by the fortuitous relationship that occurs between the vapor and liquid concentrations under equilibrium conditions. This is governed by Raoult’s law,

$$P = FP_o, \quad (1)$$

where P is the equilibrium vapor pressure in solution, P_o is the inherent vapor pressure of the pure solute, and F is the fractional saturation of the solution. By definition, this is

$$F = C/C_o \quad (2)$$

where C is the concentration of the solute (usually expressed in grams/ml) and C_o is the concentration at saturation, ie: the solubility. These two expressions can be combined and written in the form of Henry’s law,

$$P = KC, \quad (3)$$

where $K = P_o/C_o$.

“ K ” is the function which determines the partitioning of the solute between the vapor and liquid phases. For the volatile, weakly soluble substances of greatest environmental concern, K can have values three to four orders of magnitude greater than for water.

To make the infrared vapor phase measurement, it is first necessary to calibrate the system for the set of solute species likely to be present. This can be done by using one of several available multivariate quantitation approaches. The method most commonly used in the mid-IR spectral region is the “ P ” matrix approach.

In the “ P ” matrix method, the concentrations of the various species are expressed as a set of simultaneous equations involving measured absorbances in selected wavelength regions. This set of equations can be expressed in matrix form as

$$\underline{C}_G = \underline{P}\underline{A} \quad (4)$$

where \underline{C}_G is the set of gas phase molar concentrations, \underline{A} is the set of measured IR absorbances, and \underline{P} is the calibration “ P ” matrix.

The set of coefficients (matrix elements) which make up the “ P ” matrix are determined by calibrating the system using a set of samples having known concentrations.

Infrared quantitative analysis provides a measure of the vapor pressure rather than vapor phase concentration that is directly related to liquid phase concentration. We thus must make use of the ideal gas law:

$$P = C_GRT \quad (5)$$

where $C_G = n/V$.

Here, R is the universal gas constant, n is the number of moles of vapor in the gas cell, and V is the volume of the gas cell.

By combining Equation 5 with Equation 3, we obtain an expression for liquid concentration in terms of the measured vapor phase concentration:

$$C = P/K = C_GRT/K \quad (6)$$

where again K is the partitioning function.

Thus, once the vapor phase concentration of a species is determined, all that is required to determine the liquid phase



concentration is a knowledge of the temperature of the vapor in the gas cell and the value of the partitioning function, K . For most species, K will not be known in advance since the solubilities of weakly soluble substances are generally not well known. However, this uncertainty can be removed by calibrating the system with known liquid concentrations of solutes.

Continuous closed loop operation provides a rapid and robust method for on-line waste water analysis. The one weakness of this approach is the fact that the partitioning function can depend on the conditions of the waste water stream. In particular, both vapor pressure and solubility are temperature dependent and solubility can be influenced by the presence of interfering species. However, a second mode of operation is available which can determine the value of partitioning function under actual conditions of the waste stream being measured. We call this depletion rate analysis.

3. Depletion Rate Analysis

In depletion rate analysis, we sparge a static volume of water and monitor the depletion of each solute as a function of time. As will be shown below, this enables us to determine both the concentration before the onset of depletion and the partitioning function.

The depletion of solvent concentration in a static sample, as a function of time, is a simple exponential. Thus the measured vapor phase concentration has the time dependence

$$C_G(t) = C_G(0)2^{-\alpha t} \quad (7)$$

where α can be called a depletion rate constant.

The measurement of two or more points on the depletion curve allows one to determine both the initial vapor phase concentration $C_G(0)$ and the value of α .

As is shown in the appendix, the partitioning function can be obtained from the measured rate constant by using the expression,

$$K = \alpha (V_w / f)(RT / W_m) \quad (8)$$

where: V_w = water volume,

f = air flow rate,

R = 0.08206,

T = temperature of the vapor in the gas cell (°K), and

W_m = molecular weight of the solute.

Knowledge of the partitioning function enables us to determine the initial concentration of the solute in the water from the measured initial vapor concentration. By combining Equations 6 and 8, we have

$$C(0) = (C_G(0) / \alpha)(fW_m / V_w). \quad (9)$$

The significance of this method is that it enables one to measure $C(0)$ independent of P_o and C_o , and hence to eliminate the dependence of the measurement on such factors as temperature and the presence of additional solutes in the water sample.

4. Sparging-IR System Configuration

Figure 1 illustrates the benchtop sparging-IR system used to gather most of the data reported below. The key components of the system are the sparging vessel, the condenser, and the gas transmission cell. As illustrated, the system is configured for open loop operation with either a static or continuously flowing sample. For closed loop operation, we add an air pump to recirculate the air leaving the gas cell back into the input air line.

The sparging geometry is configured to provide countercurrent operation with flowing samples. This insures that the last part of the water stream encountered by the air stream will be minimally depleted by previous sparging. For most situations, the air bubbles are fine enough to enable the vapor pressure to reach equilibrium in a single pass through the vessel. When analyzing very low solubility samples in continuous flow, however, it is advantageous to use the closed loop mode so as to eliminate any net depletion of the solute in the water. Although this mode does increase the system response time, it

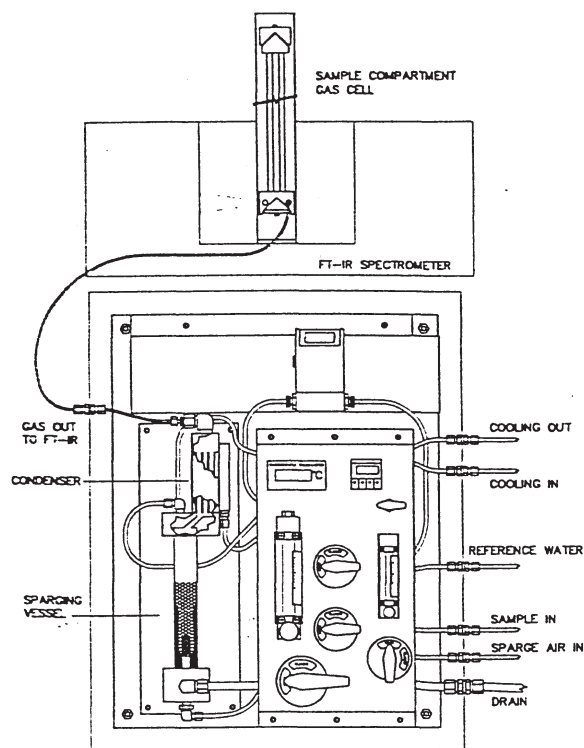


Figure 1: Physical layout of the bench top sparging-IR system.

S	C	COMPONENT NAME	Cur.	Avg.	S.D.	Max.	Min.	U	NC	LC	PTS
1	1	Carbon Tetrachloride	55.333	30.113	21.000	55.333	0.776	0.000	0.000	0.000	76
2	1	Chloroform (non)	18.028	12.022	5.342	18.015	0.144	0.000	0.000	0.000	76
3	1	Water Vapor (non)	695.922	446.887	225.857	710.325	28.624	0.000	0.000	0.000	76
4	1	Sparger Temp.	28.080	28.48	0.475	28.080	27.080	0.000	0.000	0.000	76
5	1	Water Flow (S.M)	6.430	6.23	0.205	6.080	5.180	0.000	0.000	0.000	76
6	1	Single Beam (S.M)	92.161	92.058	0.066	92.210	91.938	0.000	0.000	0.000	76

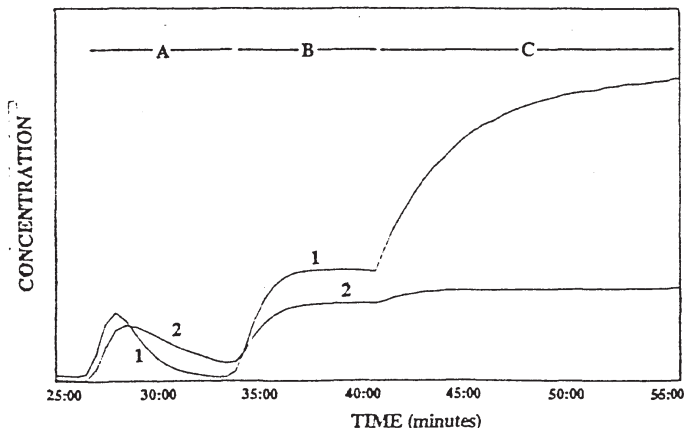


Figure 2: Typical output plot obtained using the large scale sparging-IR system. Curves 1 and 2 correspond to the measured concentrations of carbon tetrachloride and chloroform, respectively. The three distinct regions of the time history correspond to (A) open loop sparging of a static sample, (B) open loop sparging of a flowing sample, and (C) closed loop sparging of a flowing sample.

also eliminates any dependence on air or water flow rate.

The condenser, which incorporates a set of Peltier coolers, is held at a constant temperature a few degrees above freezing (typically $5.0 \pm 0.1^\circ\text{C}$). This removes significant fraction of the water vapor from the sparging air stream while holding the residual water vapor at a constant level corresponding to the dew point established by the condenser. The reduction of water vapor pressure adds an additional factor to the sensitivity enhancement already provided by dependence of the partitioning function on vapor pressure and solubility. In addition, by maintaining water vapor at a constant level, we can enhance our ability to ratio the water bands out of the spectra acquired. All of these factors, combined, can lead to a four to five order of magnitude enhancement of the ability to measure organic concentrations in water compared to a measurement in the liquid state.

The bench top sparging system uses a small light guide gas cell mounted in the FT-IR spectrometer sample compartment. The gas cell used for the tests reported below had a path length of 80 cm and a volume of 40 ml. Since the tubular nature of the cell provides essentially plug flow, its response to changes in vapor concentration is extremely fast.

The on-line version of the sparging-IR system is conceptually similar to the bench top system but much larger in scale. In this case, the gas cell has typically a two meter path length and is mounted internal to the system enclosure along with the interferometer portion of the spectrometer. The sample and air lines are considerably larger in diameter so as to handle

high flow rates and particularly dirty streams.

5. Performance Examples

Figure 2 illustrates a typical readout of the large scale sparging-IR system monitoring the concentrations of two solutes: carbon tetrachloride and chloroform. The block at the top lists the variables that are being displayed along with some statistical information and the values of the display limits. These limits can be set at any desired values, with different values for each variable. In this illustration, as well as the other illustrations which follow, the units displayed for the two solutes are ppm concentration in the gas phase. In a routine installation, the results would typically be displayed as liquid phase concentrations.

For the experiment illustrated in Figure 2, we circulated water through the sparging system from a twenty gallon tank. The water in the tank was initially spiked with approximately 350 ppb each of carbon tetrachloride and chloroform. The three regions of the time history correspond to three different operating conditions. First the sparging vessel was filled with a sample of contaminated water and then closed off. Sparging air was turned on at approximately 25:00. The initial rise time of the concentration plot corresponds roughly to time required for the leading edge of the sample to traverse the gas cell. This is followed by an exponential decay as the solutes are removed from the water by the sparging process. The difference between the decay rates for the two solutes is the result of their different solubilities and vapor pressures.

The region of the concentration plot starting at 33:00 and 40:00 correspond to open loop and closed loop operation respectively with continuous water flow in each case. In closed loop operation, the same air sample is continuously sparged through the water stream so that it eventually reaches a condition in which the vapor pressures are in equilibrium with the concentrations of the solutes in the incoming undepleted water system. At this point, the calibration is independent of the flow rates of both air stream and the waste water stream, depending only on the physical properties of the sample and the path length of the gas cell.

In open loop operation, the system response time is faster since the measurement is made in a single pass. However, the equilibrium value of measured concentration will typically be lower due to the partial depletion of solute in the water stream. This effect is most pronounced for very weakly soluble substances such as CCl_4 . It can be minimized by maximizing the ratio of water flow rate to air flow rate. In general, however, open loop operation of the large scale system requires monitoring the flow rates and correcting the system calibration for their ratio.



For the data given in Figure 2, the water and air flow rates were limited by the capacities of the pumps being used. The response speed of the system could be increased substantially by increasing the air flow rate. Also, the required calibration correction for open loop operation could be reduced by increasing the water flow rate for a given air flow rate.

Figure 3 illustrates closed loop operation of the bench top system. In this case, the water was circulated through the sparging vessel from a twenty liter reservoir. Samples of ten solutes were sequentially injected into the reservoir during the run. Since the vertical scale corresponds to gas phase concentration, the values obtained for a given liquid concentration are a measure of the partitioning functions for the various species. The measurement time resolution for this example was 13 seconds.

As can be seen from this figure, the response of the bench top system, for our operating conditions, was much faster than that of the large scale system. This is primarily a result of a much smaller air path volume. The decay in measured concentration after the initial peak is a result of the small reservoir used combined with the fact that the circulating water system was not air tight. The most important point illustrated by this data is the fact that the cross talk between the measurement channels can be minimal, even with a ten component matrix.

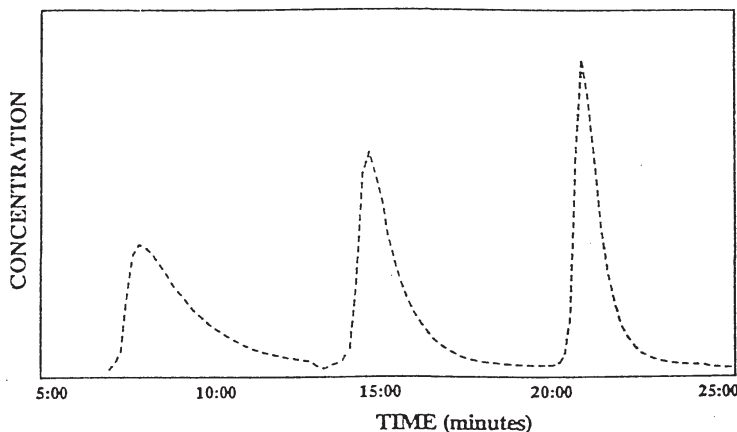
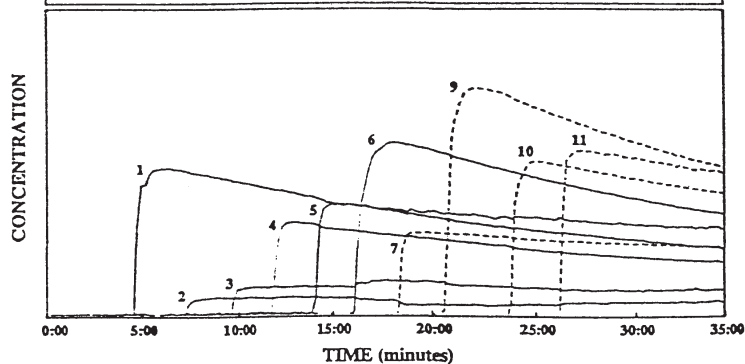
Figure 4 illustrates static sample operation with the same ten components as the closed loop measurement of Figure 3. In this case, the liquid phase concentrations were set at 2 ppm. As expected, the substances seen in Figure 3 to have the largest partitioning functions are found in Figure 4 to have the fastest depletion rates. For most of the solutes, the measured peak concentration values are comparable to those obtained in the closed loop case (Figure 3). This is due to the small air volume in the system and the fact that the depth of the water is sufficient to allow the vapor pressure to reach equilibrium in a single pass through the vessel.

Figure 5 illustrates the fact that sparging-IR measurements are dependent on temperature. The static sample depletion curves correspond to 4 ppm of chloroform in water at three different temperatures. The difference between curves is primarily due to the increase in vapor pressure with temperature, which leads to an increase in the partitioning function. This, in turn, leads to an increase in both the peak vapor concentration and the depletion rate.

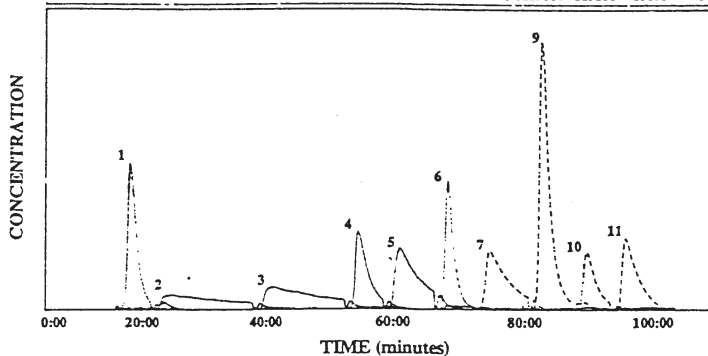
The values of the initial concentration and the depletion rate constant can be determined graphically by plotting the depletion curves on a semilog scale. This is shown in Figure 6 for the data of Figure 5.

To obtain a value for the initial gas phase concentration, we extrapolate the depletion curve back to the point where the leading edge of the absorbing sample has

S	C	COMPONENT NAME	Cur.	Avg.	S. D.	Max.	Min.	UCL	NCL	LCL	PTS.
1	1	111-Trichloroethane	14.540	19.499	8.240	32.532	-0.304	80.000	30.000	0.000	173
2	1	112-Trichloroethane	2.625	2.418	1.448	4.217	-0.611	80.000	30.000	0.000	173
3	1	12-Dichloroethane	5.814	4.251	3.194	7.853	-0.118	80.000	30.000	0.000	173
4	1	1,1-Dichloroethylene	11.378	10.211	7.586	20.332	-0.028	80.000	30.000	0.000	173
5	1	cis-Dichloroethylene	18.797	12.833	10.427	24.361	-0.023	80.000	30.000	0.000	173
6	1	Carbon Tetrachloride	22.250	13.860	13.291	38.163	-0.002	80.000	30.000	0.000	173
7	1	Chloroform	14.818	7.313	8.934	18.144	-0.226	80.000	30.000	0.000	173
8	1	Methanol	7.647	3.721	2.587	8.130	-0.708	500.000	250.000	50.000	173
9	1	Perchloroethylene	32.483	18.777	20.447	50.215	-0.100	80.000	30.000	0.000	173
10	1	Trichloroethylene	28.785	8.339	14.217	34.018	-0.317	80.000	30.000	0.000	173
11	1	1,1-Dichloroethane	31.225	4.586	10.676	30.462	-0.712	80.000	30.000	0.000	173



S	C	COMPONENT NAME	Cur.	Avg.	S. D.	Max.	Min.	UCL	NCL	LCL	PTS.
1	1	111-Trichloroethane	-0.219	1.150	7.183	83.951	-0.510	120.000	80.000	0.000	443
2	1	112-Trichloroethane	0.032	0.981	1.828	8.540	-1.382	120.000	80.000	0.000	443
3	1	12-Dichloroethane	0.141	1.318	2.586	10.135	-2.844	120.000	80.000	0.000	443
4	1	1,1-Dichloroethylene	0.470	1.181	4.308	34.851	-0.295	120.000	80.000	0.000	443
5	1	cis-Dichloroethylene	1.208	1.860	4.482	27.444	-0.715	120.000	80.000	0.000	443
6	1	Carbon Tetrachloride	0.048	1.040	3.807	58.110	-0.177	120.000	80.000	0.000	443
7	1	Chloroform	0.385	1.232	4.353	26.574	-0.487	120.000	80.000	0.000	443
8	1	Methanol	-18.863	-13.820	14.353	-2.026	-78.945	500.000	400.000	300.000	443
9	1	Perchloroethylene	0.518	0.888	13.507	120.731	-0.140	120.000	80.000	0.000	443
10	1	Trichloroethylene	-0.152	0.758	3.285	26.241	-0.351	120.000	80.000	0.000	443
11	1	1,1-Dichloroethane	-0.870	-0.006	4.780	32.554	-2.873	120.000	80.000	0.000	443



reached the mid point of the IR gas cell. To a reasonable approximation, this corresponds to the point to the left of the intersection of the two straight lines where the value of the leading edge lines is one half of the corresponding value of the

depletion line.

The Table superimposed on Figure 6 gives the inferred initial concentration values and depletion rate constants for the three temperatures. Even though $C_G(0)$ and α are both highly temperature dependent, their ratios agree to within 10 percent. This is consistent with our expectation, based on Equation (9), that depletion rate analysis would provide a liquid phase concentration measurement which is independent of solubility and vapor pressure and hence of sample temperature.

As a direct test of the solubility independence predicted by Equation (9), we altered the solubility of carbon tetrachloride by introducing substantial amounts of methanol. The results, given in Figure 7, again confirm that, even though the inferred initial vapor phase concentration and the depletion rate constant can vary widely with solubility, their ratio, and hence the predicted liquid phase concentration, will remain constant.

In continuous flow closed or open loop operation, one has the option of increasing sensitivity at the expense of time resolution by simply collecting spectra for a longer period for each data point. In static sample depletion analysis, the options are not so obvious since the sample is disappearing during the measurement. Of course, the available measurement time can always be increased by choosing a lower air flow rate at the start of a measurement. But, this requires advanced knowledge that the lower rate will be needed. Another option is to stop the air flow at two or more points during the run to allow a large number of scans to be coadded. As Figure 8 illustrates, the diffusion of the sample during this "arrested decay" period will be minimal, allowing the run to be stopped and then resumed without significantly degrading the measurement.

The resolution limit of the sparging-IR system for a given pollutant is directly proportional to the partitioning function of the substance in question. As noted above, this is equal to the ratio of inherent vapor pressure to solubility. Fortunately, the substances of greatest environmental concern generally have quite low solubilities. This is at least in part due to the fact that, since these substances are not easily dissolved in water, they tend to be retained in the human body.

The overall set of sensitivities obtained for a given monitoring task will also depend on the length of the IR gas cell and type of IR detector used, the strengths of the IR absorptions, the number of species to be monitored, the extent of band overlaps, and the nature and extent of the calibration method employed.

Table I gives the two sigma resolution limits for the "P" matrix calibration used for the data given in Figures 3 and 4. The values in the Table assume a system employing closed loop operation with a one meter gas cell and a two minute measurement time.

6. Conclusions

Sparging-infrared is a new approach to the monitoring of

organic pollutants in waste water which can provide continuous on-line measurements at levels in the low part per billion range. The system response time will generally depend on the required sensitivity, with typical measurement intervals ranging from fifteen seconds to two minutes. System calibration can be quite robust, being essentially fixed by the ratioing nature of the FT-IR measurement and the fundamental characteristics of the measurement process. In addition, depletion rate analysis can be used to calibrate out any uncertainties in solubility or vapor pressure due to the condition of the waste water stream.

The primary limitation of the sparging-IR technique resides in the fact that a system must be calibrated for a predetermined finite number of substances (typically ten to fifteen). It thus is not well suited for analyzing mixtures of unknown substances. A separation technique such as gas chromatography is more appropriate for such tasks. Rather, sparging-IR is best applied within a manufacturing plant where the identities of the potential pollutants are already known. Here the technique can perform various important functions such as the detection of leaks or spills and the monitoring of remediation processes. By facilitating the control of the waste water stream within the plant it can substantially reduce the risk of discharge into the environment.

Acknowledgements

The work reported here would not have taken place without the major contributions of Sidney W. Fleming who developed the first sparging-IR system at E.I. DuPont and whose knowledge and experience provided a sound basis for our work. A second major contributor was Bruce C. McIntosh of KVB/Analect who provided the software and vapor phase calibrations and assisted in gathering some of the data reported above. The design of the sparging-IR systems is due primarily to the efforts of Norman A. Jennings and Larry Zysman of Axiom Analytical.

References

1. S.W. Fleming, B.B. Baker, and B.C. McIntosh, "On-line Analyzer for Chlorocarbons in Wastewater", Presented at the Symposium on Pollution Prevention and Measurement, Division of Environmental Chemistry, American Chemical Society, Atlanta GA, April 14-19, 1991, proceedings in press.
2. W.M. Doyle, "Analysis of Trace Concentrations of Contaminants in Water by Sparging-FT-IR", 8th International Conference on Fourier Transform Spectroscopy, Luebeck-Travemuende, Germany, Sept. 1-6, 1991, Paper Mo-0.12 Proc. SPIE, Vol. 1575, pg 199, (1991).
3. S.W. Fleming, B.C. McIntosh, and W.M. Doyle, "Continuous FT-IR Monitoring of Volatiles in Wastewater", 1991 Joint Meeting, FACSS/Pacific Conference/27th Western Regional ACS Meeting, Anaheim, CA



THE RELATIONSHIP BETWEEN THE PARTITIONING FUNCTION AND THE DEPLETION RATE CONSTANT

To simplify the analysis, we will consider a closed vessel partially filled with water containing a small amount of solute. If we allow the vapor pressure in the head space to come to equilibrium, its value will be given by Equation 3, ie:

$$P = KC$$

where, again C is the liquid concentration and K is the partitioning function.

We next imagine that we have adjusted the head space volume until, at equilibrium, the number of molecules of solute in the vapor state are equal to the number in solution. We call this adjusted head space volume the “half depletion air volume”, V_h .

To determine the value of the half depletion volume, we first consider the ideal gas law,

$$PV = nRT,$$

where V is volume, n is the number of moles present, R is the universal gas constant, and T is temperature. This gives us the number of moles solute in the vapor phase for our assumed conditions

$$n_G = PV_h/RT = KCV_h/RT. \quad (I-1)$$

In the liquid phase, the number of moles present is by definition

$$n_L = W/W_m \quad (I-2)$$

where W is the total weight of the solute present and W_m is its molecular weight. This can be written in terms of the concentration C (in g/ml) and water volume V_w , ie:

$$n_L = CV_w/W_m \quad (I-3)$$

For the half depletion condition, $n_G = n_L$. Thus, combining Equations I-1 and I-3, we obtain

$$V_h = V_w RT/W_m K. \quad (I-4)$$

Note that the solute concentration does not appear in this equation. Thus, the half depletion volume will be the same no matter what the concentration is when we start the measurement. This condition leads directly to the exponential dependence of concentration on time.

Although the above expression was derived for a static equilibrium condition, it can be applied to the sparging case under the assumptions that the liquid is continuously mixed and that the vapor pressure reaches equilibrium before the bubbles reach the surface of the water.

For a fixed flow rate, f , the volume of air flowing through the vessel in time “ t ” will be equal to $V = ft$. Therefore, the half depletion volume of air will pass through the sparging vessel in a time, t_h , given by:

$$t_h = V_h/f \quad (I-5)$$

If we substitute this time in Equation 7 and set $C_G(t) = C_G(0)/2$ we have

$$1/2 = 2^{-\alpha t_h} \text{ or } \alpha = 1/t_h \quad (I-6)$$

Combining equations I-4, I-5, and I-6 and solving K , yields:

$$K = \alpha (V_w/f)(RT/W_m). \quad (I-7)$$